

This document is the Accepted Manuscript version of a Published Work that appeared in final form in Nano Letters, copyright © 2015 American Chemical Society after peer review and technical editing by the publisher.

To access the final edited and published work see

<https://pubs.acs.org/doi/10.1021/acs.nanolett.5b03781>

Thermal rectification by design in telescopic Si nanowires

Xavier Cartoixà,[†] Luciano Colombo,[‡] and Riccardo Rurali^{*,§}

Departament d'Enginyeria Electrònica, Universitat Autònoma de Barcelona, 08193 Bellaterra, Barcelona, Spain, Dipartimento di Fisica, Università di Cagliari, Cittadella Universitaria, 09042 Monserrato (Ca), Italy, and Institut de Ciència de Materials de Barcelona (CSIC), Campus de Bellaterra, 08193 Bellaterra, Barcelona, Spain

E-mail: rrurali@icmab.es

Abstract

We show that thermal rectification by design is possible by joining/growing Si nanowires (SiNWs) with sections of appropriately selected diameters (i.e. telescopic nanowires). This is done, first, by showing that the heat equation can be applied at the nanoscale (NW diameters down to 5 nm): we a) obtain thermal conductivity *vs.* temperature, $\kappa(T)$, curves from molecular dynamics (MD) simulations for SiNWs of three different diameters, then b) we conduct MD simulations of a telescopic NW built as the junction of two segments with different diameters, and afterwards c) we verify that the MD results for thermal rectification in telescopic NWs are very well reproduced by the heat equation with $\kappa(T)$ of the segments from MD. Second, we apply the heat equation to predict the amount of thermal rectification in a variety of telescopic SiNWs with segments made from SiNWs where $\kappa(T)$ has been experimentally

*To whom correspondence should be addressed

[†]Universitat Autònoma de Barcelona

[‡]Università di Cagliari

[§]Institut de Ciència de Materials de Barcelona

Thermal rectification by design in telescopic Si nanowires

Xavier Cartoixà,[†] Luciano Colombo,[‡] and Riccardo Rurali^{*,¶}

Departament d'Enginyeria Electrònica, Universitat Autònoma de Barcelona, 08193 Bellaterra, Barcelona, Spain, Dipartimento di Fisica, Università di Cagliari, Cittadella Universitaria, 09042 Monserrato (Ca), Italy, and Institut de Ciència de Materials de Barcelona (CSIC), Campus de Bellaterra, 08193 Bellaterra, Barcelona, Spain

E-mail: rrurali@icmab.es

Abstract

We show that thermal rectification by design is possible by joining/growing Si nanowires (SiNWs) with sections of appropriately selected diameters (i.e. telescopic nanowires). This is done, first, by showing that the heat equation can be applied at the nanoscale (NW diameters down to 5 nm): we a) obtain thermal conductivity vs. temperature, $\kappa(T)$, curves from molecular dynamics (MD) simulations for SiNWs of three different diameters, then b) we conduct MD simulations of a telescopic NW built as the junction of two segments with different diameters, and afterwards c) we verify that the MD results for thermal rectification in telescopic NWs are very well reproduced by the heat equation with $\kappa(T)$ of the segments from MD. Second, we apply the heat equation to predict the amount of thermal rectification in a variety of telescopic SiNWs with segments made from SiNWs where $\kappa(T)$ has been experimentally

*To whom correspondence should be addressed

[†]Universitat Autònoma de Barcelona

[‡]Università di Cagliari

[¶]Institut de Ciència de Materials de Barcelona

measured, obtaining r values up to 50%. This methodology can be applied to predict the thermal rectification of arbitrary heterojunctions as long as the $\kappa(T)$ data of the constituents are available.

Thermal diodes are systems whose thermal resistance depends on the sign of the applied thermal gradient and where, accordingly, heat current preferentially flows in one direction.¹⁻³ These devices are one of the key building blocks of phononics, the discipline that investigates the manipulation of heat with the goal to engineer devices with the same functionalities as electrical diodes and transistors.⁴

In semiconductors, where heat is mostly carried by phonons, thermal rectification can be achieved in heterostructures made of materials whose thermal conductivity κ has a different dependence on the temperature⁵⁻⁹ or in graded systems.¹⁰ These systems should fulfill at least two requirements. The first and most important one is that the temperature dependence of κ of the two materials be sufficiently different to produce a sizeable rectification.⁸ The second condition is that the junction should have a low enough interface thermal resistance (ITR): a large ITR would dominate the overall thermal resistance and, therefore, would mask the asymmetric temperature response of the two materials.⁹ This last requirement can be partly cast aside by increasing the length, so that the relative weight of the ITR vanishes, but would otherwise limit the choice to materials that can form low ITR, epitaxial junctions.

Nanostructures offer in principle a workaround to these limitations. On one hand, nanostructuring allows tuning several properties of a material, and thermal conductivity is no exception. It has been shown experimentally, for instance, that in Si nanowires¹¹ with a diameter of 22 nm κ increases monotonously as the temperature increases, while in nanowires thicker than 56 nm it first reaches a maximum and then, when phonon-phonon scattering dominates, it decreases (the expected behavior of a large class of bulk materials).¹² On the other hand, the lateral release of strain makes epitaxial junctions of mismatched lattices possible, like in the case of Si-Ge nanowires.¹³

In this Letter we explore thermal transport and thermal rectification in *telescopic* silicon nanowires (SiNWs), i.e. nanowires with an abrupt variation of diameter. To do so, we first show that molec-

ular dynamics (MD) thermal transport results for SiNWs of a few nm in diameter are very well reproduced by the heat equation when consistent $\kappa(T)$ data are provided. Then we apply the heat equation, thus avoiding time-consuming non-equilibrium MD simulations, to predict the thermal rectification of telescopic SiNWs built from segments where experimental $\kappa(T)$ curves are available

Telescopic nanowires have been produced experimentally both from Si^{14,15} and III-Vs,¹⁶ and they can be in principle also obtained by state-of-the-art lithographic techniques. Lateral confinement modifies the phonon density of states as a function of NW thickness, and the combination of NWs of different diameters paves the way to thermal rectifiers by design.

In order to validate the use of the heat equation at the nanoscale, with its very large temperature gradients associated and a perhaps significantly large fraction of ballistic phonons, which cast doubts about its validity, we first perform a series of numerical experiments designed to a) obtain $\kappa(T)$ curves, and b) obtain values of the thermal rectification from an atomistic thermal transport description. Thus, we perform non-equilibrium molecular dynamics (NEMD) simulations with the LAMMPS code,¹⁷ using a Stillinger-Weber potential,¹⁸ reparameterized with a first-principles-based force-matching method.^{19,20} Although classical potentials are not quantitatively very accurate,²¹ this is of no concern for this work as the NEMD results are used either to calculate the thermal rectification –which relies on relative differences of the forward and reverse conductivity– or to provide results against which to validate the predictions of the heat equation. We have not terminated the surface dangling bonds with hydrogens as it was previously shown that they do not affect the estimate of the thermal conductivity.²² All our NEMD simulations in this work involve 5, 10 and 15 nm diameter SiNWs grown along the [111] direction, taken to be the z coordinate direction (see Figure 1). The ends of the NWs are connected to Nosé-Hoover thermostats at temperatures T_L and T_R , while the atoms between the two reservoirs evolve according to Newton’s equations of motion without any thermostating from an initial temperature of $(T_L + T_R)/2$. The thermal gradient builds up across the nanowire because of the contact with the two thermostats. We calculate the heat current as the energy per unit of time that the thermal

reservoirs have to inject/extract to maintain the imposed $\Delta T = T_L - T_R$. In the non-equilibrium steady-state, the difference between these two heat currents is within the 0.5 %, which we consider to be a good indication that the system has reached a stationary state. We consider ΔT from ± 50 K to ± 400 K, with $(T_L + T_R)/2 = 300$ K throughout the paper, performing $7.5 \cdot 10^6$ NEMD steps with a timestep of 0.7 fs and estimating the heat current in the last $3 \cdot 10^6$ steps.

$\kappa(T)$ — Before tackling our telescopic junctions, we studied the dependence of κ on the temperature of Si NWs with a uniform diameter. Our tests showed that the estimate of $\kappa(T)$ is rather insensitive to the imposed ΔT . Yet, while in principle small gradients are more suited to the evaluation of an equilibrium property in the linear response regime (Fourier regime), i.e. $\kappa(T)$, a ΔT of at least 50 K ($\nabla T = 0.93$ K/nm) is necessary for sufficiently noise-free heat currents; we used $\Delta T = 100$ K. The results for the 5 and the 10 nm NW are shown in Figure 2a. Thermal conductivities are calculated from Fourier’s law from the effective ∇T in the central region of the NW and the calculated heat current. The functional shapes of the two $\kappa(T)$ curves are rather similar, but the 10 nm NW has a conductivity that is roughly 1.6 times larger, all over the temperature range investigated. The fact that a narrower NW has a lower conductivity is a clear fingerprint of the strong effect of boundary scattering in microscopic heat carriers and agrees with previous theoretical^{23–25} and experimental¹² results.

ITR and rectification with NEMD — Next, we study telescopic junctions made of the previously studied 5, 10 and 15 nm diameter SiNWs segments. The overall length of the wires is ~ 60 nm and the interface is assumed to have a vanishing thickness and to be located where the diameter changes. Specifically, we first look at the ITR and its dependence on ΔT of the 5-10 nm telescopic NWs. We calculate the ITR by estimating the thermal discontinuity at the interface, ΔT_i , and dividing it by the heat current.²⁶ The temperature profile along the NW axis for $\Delta T = 400$ K is shown in Figure 2b. Notice how the 5 nm NW, on the left side of the junction, experiences a larger thermal gradient than the 10 nm NW, as expected from its larger resistivity (see Figure 2a). We repeated the same analysis for different values of ΔT , finding that the ITR decreases with the applied thermal bias. This result stems from the dependence of the interface temperature –

defined as the mean value of the temperature discontinuity²⁷– on ΔT (black spheres in Figure 2c). Neglecting the ITR and treating the system as a simple temperature divider, in analogy with the more common voltage divider, it is easy to show that the interface temperature is

$$T_i = \frac{T_L + T_R}{2} + \frac{R_R - R_L}{2(R_L + R_R)}\Delta T \quad (1)$$

where R_L and R_R are the thermal resistances of the NW on the left and on the right side of the junction, respectively. Therefore, T_i is the average of the temperatures of the reservoirs only for vanishingly small ΔT or if $R_R = R_L$. In our case, where $R_L > R_R$, a decrease of the interface temperature is expected and, indeed, observed in the NEMD calculations (see Figure 2c). Notice that the decrease is not linear, because R_L and R_R depend on the T profile, which in turn depends on T_i . It is useful to stress once again that the constituent material and the direction along which heat flows –Si and the [111] axis, respectively– are the same for the 5 and the 10 nm NW, thus both the ITR and the difference in thermal conductivity derive exclusively from the different degree of confinement. Introducing different chemical species, e.g. a SiGe axial or core-shell telescopic nanowire, would add an additional degree of freedom in the design of the thermal transport properties.

We now focus on the thermal rectification of the telescopic NWs of Figure 1 by running a series of NEMD simulations for a given set of $\pm\Delta T$. We find that heat flow from thick to thin NWs is favored. Rectification, defined as

$$r = \frac{|I_{\text{thick} \rightarrow \text{thin}}| - |I_{\text{thin} \rightarrow \text{thick}}|}{|I_{\text{thin} \rightarrow \text{thick}}|} \quad (2)$$

where $I_{\text{thick} \rightarrow \text{thin}}$ ($I_{\text{thin} \rightarrow \text{thick}}$) is the heat current when phonons flow from a thick (thin) to a thin (thick) NW, originates from the different temperature dependence of κ of the thick and thin segments of the telescopic junction that we have discussed above for the 5 and 10 nm NWs. Simply put, $R_5^{\text{hot}} + R_{10}^{\text{cold}} > R_5^{\text{cold}} + R_{10}^{\text{hot}}$, where R_D^{cold} (R_D^{hot}) is the thermal resistance of a NW of diameter D connected to a cold (hot) reservoir. The results are summarized in Figure 3. We obtain the largest rectification from a junction made of a 10 and a 15 nm SiNW, which is of the order of the

largest experimental values reported to date^{28,29} at $\Delta T = 100$ K and has a peak value of 15 % for larger gradients. The other telescopic NWs have a rectifying behavior similar to what we reported previously of Si-Ge NW axial junctions.⁹

Heat equation validation — The overall thermal resistance can be written as

$$R_{tot} = \int_0^{L/2} \frac{1}{S_A} \rho_A [T(z)] dz + R_i(T_i) + \int_{L/2}^L \frac{1}{S_B} \rho_B [T(z)] dz \quad (3)$$

where $\rho_{A,B} = \kappa_{A,B}^{-1}$ and $S_{A,B}$ are the thermal resistivities and the cross-sections of materials A and B (wires of different diameters), and R_i is the ITR. It is easy to see that, for a given pair of materials, R_{tot} depends exclusively on the temperature profile along the wire axis, $T(z)$, which is determined self-consistently by the thermal bias and by $\kappa(T)_{A,B}$. Therefore, we have implemented a finite element solver of the heat equation to calculate $T(z)$ along a telescopic Si NW. The heat equation in its general form reads as

$$c_v \delta \frac{\partial T(\mathbf{r}, t)}{\partial t} = \nabla \cdot [\kappa \nabla T(\mathbf{r}, t)] + q(\mathbf{r}, t) \quad (4)$$

where c_v is the specific heat capacity, δ is the mass density and q is a heat source. In the stationary one-dimensional case it becomes:

$$\frac{\partial}{\partial z} \left[S(z) \kappa(z) \frac{\partial T(z)}{\partial z} \right] + S(z) q(z) = 0 \quad (5)$$

The solution obtained for $\Delta T \sim 150$ K and its very good agreement with the T profile directly obtained from a NEMD simulation is shown in Figure 4. A pair of delta shaped heat sources at the junction, $\bar{q} \delta(L/2^-)$ and $-\bar{q} \delta(L/2^+)$, can be tuned to account for the ITR and further improve the agreement. The importance of this result is twofold: (i) it indicates that the heat equation can be safely applied to these deeply scaled nanowires; and (ii) it allows predicting the thermal rectification of a heterojunction whenever $\kappa(T)$ –either theoretically calculated or experimentally measured– is available for a pair of materials. Thus, NEMD runs that are time-consuming or just

beyond current computational capabilities can be avoided. Similarly, Dames⁸ showed that in the case of thermal conductivities with power-law temperature dependencies, the maximum thermal rectification can be expressed as a function of the thermal bias and of the difference $n_1 - n_2$, the exponents of the $\kappa(T) \propto T^n$ curves of the two materials. Our approach, however, is more general, because it is not restricted to a power law dependence of $\kappa(T)$ (or to a temperature range where there is such power law dependence; for instance the in-plane conductivity of graphite is well described by a T^n curve, but the exponent n changes from 2 to -1.1 around 100 K⁸).

Thermal rectification prediction — As an example of the considerations above, we take the conductivity measurements of 22, 37, and 56 nm SiNWs reported by Li *et al.*,¹² and we solve the heat equation under different thermal gradients, for 22-37 nm, 22-56 nm and 37-56 nm telescopic junctions. We notice that the thermal conductivities measured by Li *et al.*¹² are not fully satisfactorily fitted to a T^n dependence, and low temperature deviations from the Debye T^3 law have been reported for the 22 nm NW, thus emphasizing the advantage of our approach. We calculate the thermal resistance from 3 for $\pm\Delta T$ and estimate the heat rectification from 2. The results are plotted in Figure 5. We have obtained the largest rectifications by combining 37 and 56 nm Si NWs, with peak values around 50 % when one of the ends of the telescopic wire is at very low temperature.

Conclusions — In conclusion, we have performed non-equilibrium molecular dynamics (NEMD) calculations of thermal transport in telescopic Si nanowires, we have verified that a numerical solution of the heat equation reproduces very well the NEMD results in these systems, and then we have predicted with the heat equation the amount of thermal rectification that can be expected from joining SiNWs of different diameters where $\kappa(T)$ curves have been experimentally measured.¹² As the thermal conductivity and its temperature dependence $\kappa(T)$ vary with the nanowire diameter, these systems constitute a good proof-of-concept of thermal rectification by design, where the rectification and other important parameters such as the interface thermal resistance can be tuned by joining NWs of different thickness in a telescopic junction.

Acknowledgement

We acknowledge funding under contracts Nos. FIS2012-37549-C05-05, TEC2012-31330, TEC2012-32305, MAT2013-40581-P, and CSD2007-00041 (partially funded by the FEDER program of the EU) of the Ministerio de Economía y Competitividad (MINECO).

References

- (1) Terraneo, M.; Peyrard, M.; Casati, G. *Phys. Rev. Lett.* **2002**, *88*, 094302.
- (2) Li, B.; Wang, L.; Casati, G. *Phys. Rev. Lett.* **2004**, *93*, 184301.
- (3) Roberts, N.; Walker, D. *Int. J. Therm. Sci.* **2011**, *50*, 648–662.
- (4) Li, N.; Ren, J.; Wang, L.; Zhang, G.; Hänggi, P.; Li, B. *Rev. Mod. Phys.* **2012**, *84*, 1045–1066.
- (5) Marucha, C.; Mucha, J.; Rafałowicz, J. *Phys. Stat. Sol. (a)* **1975**, *31*, 269–273.
- (6) Balcerek, K.; Tyc, T. *Phys. Stat. Sol. (a)* **1978**, *47*, K125–K128.
- (7) Jeżowski, A.; Rafalowicz, J. *Phys. Stat. Sol. (a)* **1978**, *47*, 229–232.
- (8) Dames, C. *J. Heat Transfer* **2009**, *131*, 061301–061301.
- (9) Rurali, R.; Cartoixà, X.; Colombo, L. *Phys. Rev. B* **2014**, *90*, 041408.
- (10) Wang, J.; Pereira, E.; Casati, G. *Phys. Rev. E* **2012**, *86*, 010101.
- (11) Rurali, R. *Rev. Mod. Phys.* **2010**, *82*, 427–449.
- (12) Li, D.; Wu, Y.; Kim, P.; Shi, L.; Yang, P.; Majumdar, A. *Appl. Phys. Lett.* **2003**, *83*, 2934–2936.
- (13) Amato, M.; Palummo, M.; Rurali, R.; Ossicini, S. *Chem. Rev.* **2014**, *114*, 1371–1412.
- (14) Kamins, T. I.; Li, X.; Williams, R. S. *Appl. Phys. Lett.* **2003**, *82*, 263–265.
- (15) Christesen, J. D.; Pinion, C. W.; Grumstrup, E. M.; Papanikolas, J. M.; Cahoon, J. F. *Nano Lett.* **2013**, *13*, 6281–6286.
- (16) Priante, G.; Ambrosini, S.; Dubrovskii, V. G.; Franciosi, A.; Rubini, S. *Cryst. Growth Des.* **2013**, *13*, 3976–3984.
- (17) Plimpton, S. *J. Comp. Phys.* **1995**, *117*, 1–19.

- (18) Stillinger, F. H.; Weber, T. A. *Phys. Rev. B* **1985**, *31*, 5262–5271.
- (19) Lee, Y.; Hwang, G. S. *Phys. Rev. B* **2012**, *85*, 125204.
- (20) Lee, Y.; Hwang, G. S. *J. Appl. Phys.* **2013**, *114*, 174910.
- (21) He, Y.; Savić, I.; Donadio, D.; Galli, G. *Phys. Chem. Chem. Phys.* **2012**, *14*, 16209–16222.
- (22) Markussen, T.; Jauho, A.-P.; Brandbyge, M. *Nano Lett.* **2008**, *8*, 3771–3775.
- (23) Volz, S. G.; Chen, G. *Appl. Phys. Lett.* **1999**, *75*, 2056–2058.
- (24) Wang, J.; Wang, J.-S. *Appl. Phys. Lett.* **2007**, *90*, 241908.
- (25) Wang, S.-c.; Liang, X.-g.; Xu, X.-h.; Ohara, T. *J. Appl. Phys.* **2009**, *105*, 014316.
- (26) Landry, E. S.; McGaughey, A. J. H. *Phys. Rev. B* **2009**, *80*, 165304.
- (27) Other definitions of the interface temperature are possible and rely on a non vanishing thickness of the interface itself, thus allowing calculating the mean temperature on a suitable set of atoms. Different choices could result in some quantitative difference, but are not expected to alter the overall physical picture.
- (28) Chang, C. W.; Okawa, D.; Majumdar, A.; Zettl, A. *Science* **2006**, *314*, 1121–1124.
- (29) A significantly larger value has been reported very recently in a metal-superconductor system,³⁰ although in that case it was the electronic, rather than the phononic heat current to be rectified.
- (30) Martínez-Pérez, M. J.; Fornieri, A.; Giazotto, F. *Nature Nanotech.* **2015**, *10*, 303–307.

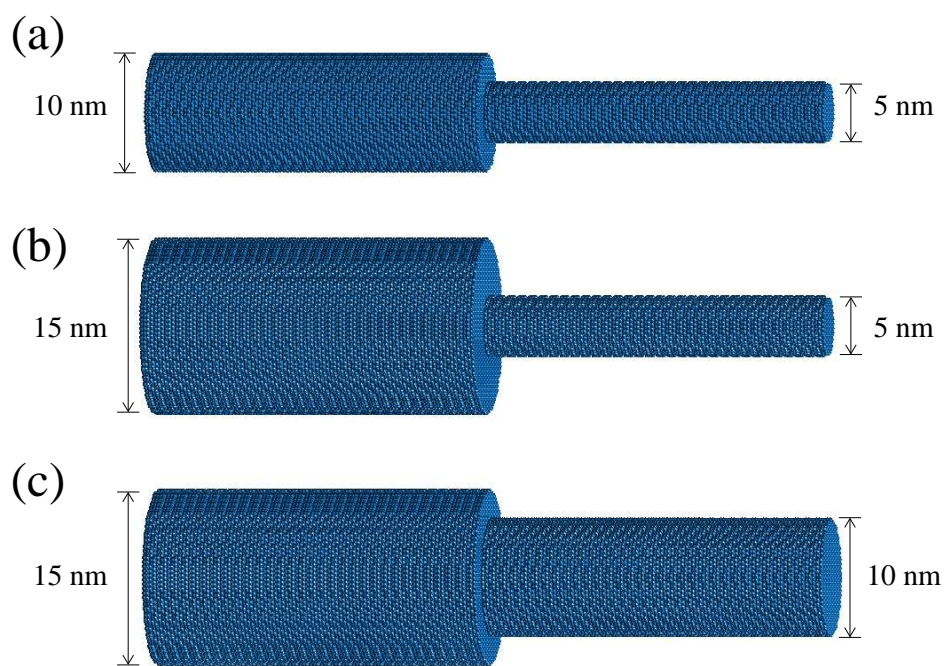


Figure 1: Telescopic Si NWs obtained joining individual wire of (a) 5 and 10 nm, (b) 5 and 15 nm, and (c) 10 and 15 nm.

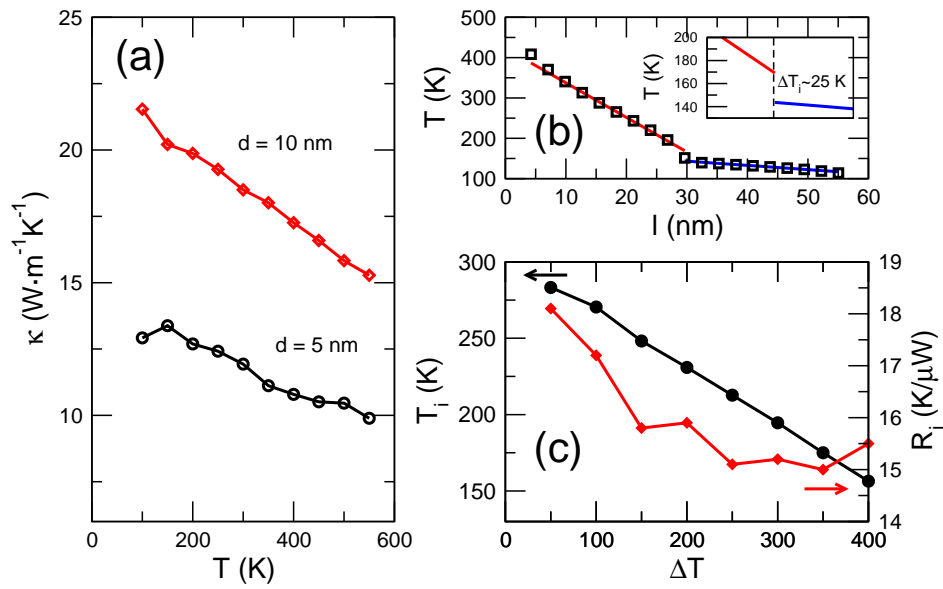


Figure 2: The 5-10 nm telescopic junctions. (a) Thermal conductivity as a function of temperature for Si NWs with a uniform diameter of 5 and 10 nm. (b) Temperature profile along the NW axis for an applied $\Delta T = 400$ K; the discontinuity at the junction is the signature of the ITR (zoomed view in the inset). (c) ITR and interface temperature as a function of ΔT .

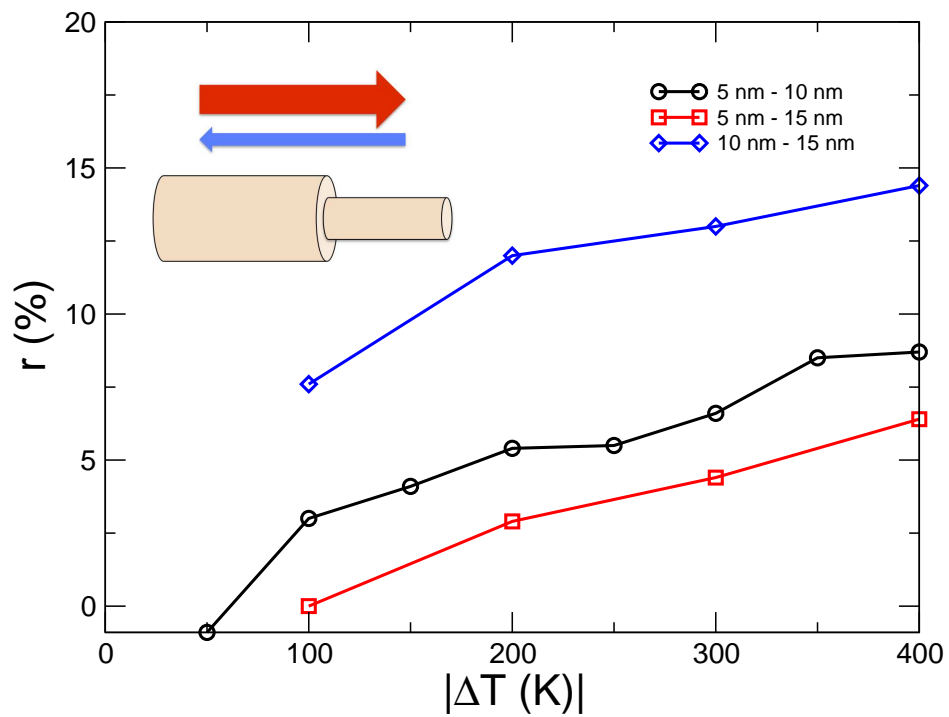


Figure 3: Thermal rectification obtained from NEMD calculations of three different telescopic Si NWs. Phonons are found to preferentially flow from the thick to the narrow NW, as schematically depicted in the inset.

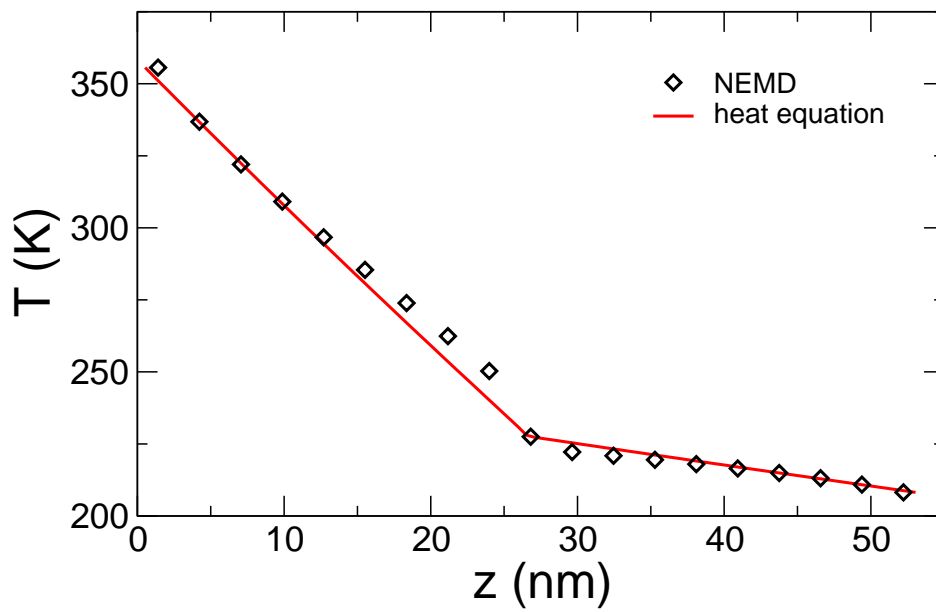


Figure 4: Temperature as a function of the axial coordinate z in a 5-10 nm telescopic junction as obtained from NEMD simulation (symbols) and from the numerical solution of 5 (continuous line) In the case of the NEMD simulations, we calculate the mean temperature of a slab perpendicular to the transport direction, like we did for the plots of Figure 2b.

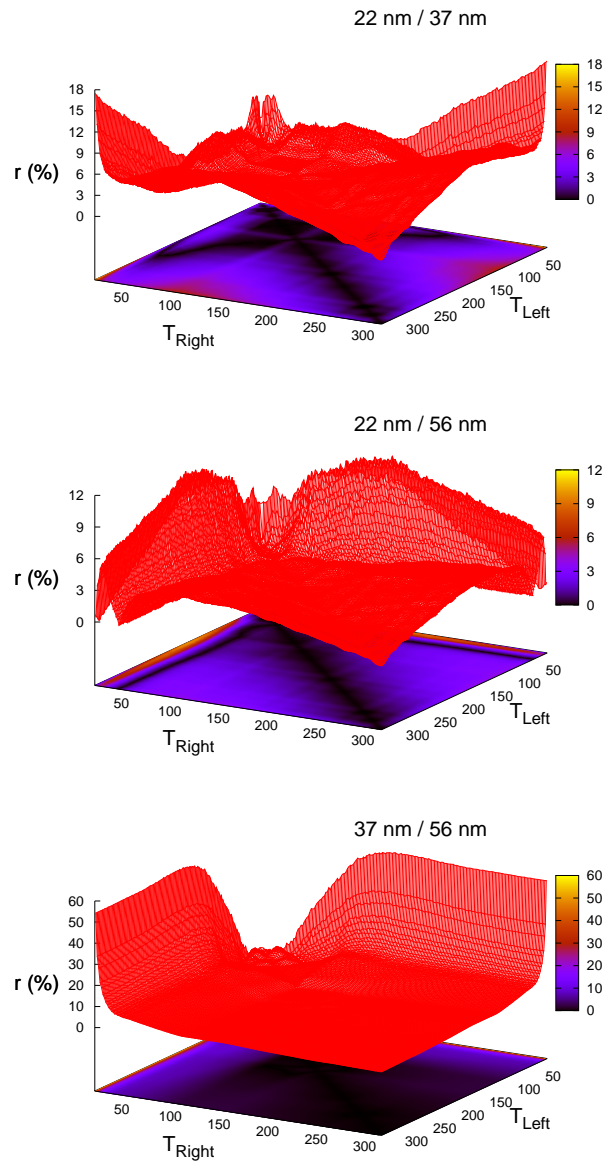


Figure 5: Thermal rectification for three telescopic Si NWs: 22-37 nm, 22-56 nm and 37-56 nm. The experimental data for 22, 37, and 56 nm Si NWs are taken from Li *et al.*¹²